

# Rapid and sensitive detection of *Mycoplasma synoviae* using RPA combined with *Pyrococcus furiosus* Argonaute

Yanli Zhao,<sup>\*,†</sup> Yuhua Zhang,<sup>\*,†</sup> Weiqing Wu,<sup>\*,†</sup> Tianhao Kang,<sup>\*,†</sup> Jian Sun,<sup>\*,†</sup> and Hongxia Jiang <sup>\*,†,1</sup>

<sup>\*</sup>Guangdong Key Laboratory for Veterinary Pharmaceuticals Development and Safety evaluation, College of Veterinary Medicine, South China Agricultural University, Guangzhou, 510642, China; and <sup>†</sup>Guangdong Laboratory for Lingnan Modern Agriculture, South China Agricultural University, Guangzhou, 510642, China

**ABSTRACT** *Mycoplasma synoviae* (MS) is an important pathogen in laying hens and causes serious economic losses in poultry production. Rapid, accurate and specific detection is important for the prevention and control of MS. Argonaute from *Pyrococcus furiosus* (*PfAgo*) is emerging as a nucleic acid detector that works via “dual-step” sequence-specific cleavage. In this study, an MS detection method combining recombinase polymerase amplification (RPA) and *PfAgo* was established. Through elaborate design and screening of RPA primers and *PfAgo* gDNA and condition optimization,

amplification and detection procedures can be completed within 40 min, whereas the results were superficially interpreted under UV and blue light. The sensitivity for MS detection was 2 copies/ $\mu$ L, and the specificity results showed no cross reaction with other pathogens. For the detection of 31 clinical samples, the results of this method and qPCR were completely consistent. This method provides a reliable and convenient method for the on-site detection of MS that is easy to operate without complex instruments and equipment.

**Key words:** *Mycoplasma synoviae*, *Pyrococcus furiosus* Argonaute, recombinase polymerase, detection

2024 Poultry Science 103:103244

<https://doi.org/10.1016/j.psj.2023.103244>

## INTRODUCTION

*Mycoplasma synoviae* (MS) infection remains a serious problem in poultry farming and can cause arthritis, tendinitis, air sacculitis, and eggshell apex abnormalities, which are responsible for substantial economic losses in poultry breeding (Kleven and Ferguson-Noel, 2008). Furthermore, MS is often coinfectd with *Escherichia coli*, infectious bronchitis virus (IBV), Newcastle disease virus (NDV), and *Mycoplasma gallisepticum* (MG); moreover, it aggravates clinical symptoms and elicits difficulties in the diagnosis of the disease (Landman and Feberwee, 2004; Sid et al., 2015). Voluntary control and eradication programs for MS have been implemented in the United States and the United Kingdom (Landman, 2014; Kaboudi K, 2019). Rapid, accurate, and sensitive detection methods are important for the clinical control and eradication of MS infections.

The isolation and identification of pathogens is the gold standard for the diagnosis of MS infection (Kleven, 2008). However, the isolation of MS is difficult and time-

consuming. Serological methods have the advantage of being fast and easy to operate but cannot timely and accurately reflect MS infection (Kleven, 1975; Luciano et al., 2011). With the development of molecular biology, PCR and quantitative polymerase chain reaction (qPCR) methods have been established for the detection of MS, usually with high sensitivity and specificity (Lauerman et al., 1993; Bashashati and Sabouri, 2022). These methods are not convenient to use in limited feeding conditions because of the need for cumbersome precision thermal cyler equipment. Additionally, isothermal amplification technology has rapidly developed in recent years, including recombinase polymerase amplification (RPA) and loop-mediated isothermal amplification (LAMP) (Kursa et al., 2015; Xia et al., 2022). The methods can be completed under constant temperature; however, the specificity is poor, and false-negatives or false-positives are easily generated. Currently, nuclease-based rapid detection methods have been established, such as Cas nucleases from CRISPR systems (Li et al., 2018; Zhou et al., 2018), Argonaute (Ago) proteins and endonuclease IV, which have been applied to nucleic acid detection (Xiao et al., 2012; Xiao et al., 2013; He et al., 2019; Chen et al., 2023). Nucleic acid targets can generate signals by activating nucleases and are highly specific; moreover, isothermal amplification is combined to improve sensitivity and operability.

© 2024 Published by Elsevier Inc. on behalf of Poultry Science Association Inc. This is an open access article under the CC BY-NC-ND license (<http://creativecommons.org/licenses/by-nc-nd/4.0/>).

Received July 30, 2023.

Accepted October 24, 2023.

<sup>1</sup>Corresponding author: [hxjiang@scau.edu.cn](mailto:hxjiang@scau.edu.cn)

Ago from *Pyrococcus furiosus* (**pfAgo**) and *Thermus thermophilus* (**TtAgo**) are most commonly applied for nucleic acid detection (Song et al., 2020; Xun et al., 2021b). *pfAgo* has the activity of targeted cleavage at 95°C. When the guide DNA (**gDNA**), which is 5'-phosphorylated ssDNA, recognizes the complementary target, it activates the *PfAgo* nuclease, whereby it specifically cleaves the target between the 10th and 11th nucleotide bases from the 5' to 3' ends of the aligned gDNA. Correspondingly, cleavage produces another ssDNA fragment with 5'-phosphorylation that can be used as a second gDNA to guide *PfAgo* for secondary cutting (Xun et al., 2021b). Ago-based detection methods cut targets in a sequence-specific manner with multi-turnover activity. In addition, a “dual-step” of specific sequence cleavage is required for detection, which can be used for nucleic acid-specific and multiplex detection (Wang et al., 2021b; Ye et al., 2022). In this study, we combined isothermal amplification of RPA and target identification of ago nucleases to establish a rapid detection method for MS. The method was completed within 40 min with high sensitivity and specificity, thus providing a reliable and convenient method for the detection of clinical MS.

## MATERIALS AND METHODS

### Bacterial Strains and Clinical Samples

The *M. synoviae* strain (WVU1853) was provided by Foshan University (Foshan, China); additionally, MS-H (commercial live attenuated vaccine strain), *Staphylococcus aureus* (ATCC 29213), *E. coli* (ATCC 25922), *Salmonella* (ATCC 14028), *Klebsiella pneumoniae* (ATCC 13883), the *M. gallisepticum* S6 strain and the *M. gallinaceum* strain were maintained in our laboratory. Clinical samples were collected from a chicken farm in Guangdong Province, and throat and choanal cleft swab samples of chickens were collected with cotton swabs and placed in PBS.

### DNA Extraction

There were 2 methods used to extract the whole genome of bacteria: the boiling method and the kit-based method. The preserved strains were resuscitated, and genomic DNA was extracted from bacterial cultures with a HiPure Bacterial DNA Kit (Magen, Guangzhou, China). DNA extraction of swab samples was performed according to a previously published method with some modifications (Bozorgmehrifard et al., 2018). The collected samples were centrifuged at  $14,000 \times g$  for 10 min; afterward, the supernatant was removed, and the precipitate was suspended in 25  $\mu$ L of ddH<sub>2</sub>O. The contents of the tube were boiled for 10 min at 100°C in a heating block, followed by an ice bath for 10 min and subsequent centrifugation at  $14,000 \times g$  for 10 min. The supernatant was transferred to a new tube as a template. The extracted nucleic acids were stored at -20°C for subsequent tests.

### Preparation of Recombinant Plasmids

The whole genome of MS was downloaded from NCBI, and the sequences were aligned with SnapGene software (California, CA). Conserved heat shock ATP-dependent protease was selected as the detection target. The 784 bp fragment was amplified via PCR by using the primers in Table S1, cloned into the pMD-19T vector (Takara, Beijing, China) after purification with a gel purification kit (Vazyme, Nanjing, China) and subsequently transformed into *E. coli* DH 5 $\alpha$  competent cells (Genesand, Beijing, China). Tsingke Biotech (Beijing, China) sequenced the recombinant plasmid pMD-19T-ATP for confirmation. Plasmids were extracted with a HiPure Plasmid Micro Kit (Magen), and the concentration was measured by using a NanoDrop ND-2000 spectrophotometer (NanoDrop Technologies, DE). The copy number of pMD-19T-ATP was calculated via the following formula:  $\text{copies}/\mu\text{L} = (6.02 \times 10^{23}) \times (\text{ng}/\mu\text{L} \times 10^{-9}) / (\text{length of DNA} \times 660)$ .

### Design of RPA Primer

To obtain the best amplification efficiency of RPA-based preamplification, according to the RPA primer design principles, the size of the amplified fragment ranged between 120-200 bp, and the length of the primer was between 25-35 bp. A total of 3 forward and 3 reverse primers were designed by using Primer Premier 5.0 (PREMIER Biosoft) according to the heat shock ATP-dependent protease genes (Table 1), and 9 sets of primers were combined in pairs for RPA primer selection. All of the oligonucleotides in this study were synthesized by Tsingke Biotech.

### Design and Screening of gDNA

A 59 bp stretch of ssDNA was synthesized in the middle of the PRA amplified sequence, and 8 complementary gDNA were designed every 4 bases. gDNAs were prepared by phosphorylating the synthesized 16 bp ssDNA using T4 polynucleotide kinase (New England Biolabs, Ipswich, MA). The 25  $\mu$ L *PfAgo* cleavage ssDNA reaction contained 2.5  $\mu$ L of  $10 \times$  reaction buffer (150 mM Tris/HCl, 1 M NaCl, pH 8.0), 0.2  $\mu$ M *PfAgo* (JiaoHong Biotech, Shanghai, China), 0.8  $\mu$ M ssDNA, 0.6  $\mu$ M gDNA and 2  $\mu$ M MnCl<sub>2</sub>; additionally, ddH<sub>2</sub>O was added to 25  $\mu$ L. After 1 h of incubation at 95°C, the product was combined with a  $2 \times$  loading buffer (Sangon, Shanghai, China) mixture and subsequently analyzed with 16% urea-denaturing PAGE in  $1 \times$  Tris–borate–ethylenediaminetetraacetic acid (TBE).

### RPA-PfAgo Assay

Recombinase polymerase amplification was performed according to the manufacturer's instructions for the DNA Rapid Amplification Kit (Amp-future; Weifang, China). Briefly, a 50  $\mu$ L reaction mixture containing

29.4  $\mu\text{L}$  of A buffer, 2  $\mu\text{L}$  of each primer (10  $\mu\text{M}$ ), 9.1  $\mu\text{L}$  of ddH<sub>2</sub>O, 5  $\mu\text{L}$  of template, and 2.5  $\mu\text{L}$  of B buffer was added to a lyophilized powder tube. The mixture was vortexed after a brief centrifugation, and the reaction was performed at 39°C for 30 min. Afterward, 3  $\mu\text{L}$  of the amplified product was added to 20  $\mu\text{L}$  of *Pf*Ago reaction mixture supplemented with 0.64  $\mu\text{M}$  *Pf*Ago, 126 nM gDNA, 2.5 mM MgSO<sub>4</sub>, 0.5  $\mu\text{M}$  molecular beacon, 2  $\mu\text{L}$  of 10  $\times$  reaction buffer and ddH<sub>2</sub>O brought up to 20  $\mu\text{L}$ . The reaction was performed in a CFX Connect Real-Time PCR Detection System (California, CA) at 95°C for 30 min, and the FAM fluorescence signal was collected once every 30 sec. When the reaction was complete, the tube was photographed by using a smartphone under blue light or analyzed via an Imaging System (Azure Biosystem, California, CA) after an exposure time for observation.

### RPA-*Pf*Ago Sensitivity and Specificity Tests

To investigate the sensitivity of the RPA-*Pf*Ago reaction, 10-fold serial dilutions of the pMD-19T-ATP plasmid standard (ranging from  $2 \times 10^8$  to  $2 \times 10^0$  copies/ $\mu\text{L}$ ), after which the dilution was doubled to 1 copy/ $\mu\text{L}$ ) were used as templates for the RPA reaction, whereas ddH<sub>2</sub>O was used as a negative control. The amplified products were used for further detection of fluorescence for *Pf*Ago cleavage. To confirm the specificity, nucleic acids from *S. aureus*, *E. coli*, *Salmonella*, *K. pneumoniae* (KPN), MG, and *M. gallinaceum* (MGC) were extracted, and MS and MS-H were used as positive controls for specific detection. After quantifying the fluorescence, images of the tubes were collected under UV and blue light.

### qPCR Reaction

qPCR primers in Table S1 were designed by using the online tool primer 3 (<https://bioinfo.ut.ee/primer3/>), and dilutions of the plasmids were used as templates to test the sensitivity. The primers in the references were used to test the clinical samples (OIE, 2008). qPCR reactions were performed with 2  $\times$  Taq Pro Universal SYBR qPCR Master Mix (Vazyme); the reaction mixture contained 5  $\mu\text{L}$  master mix, 0.2  $\mu\text{L}$  primer (10  $\mu\text{M}$ ), 1  $\mu\text{L}$  template, and the addition of ddH<sub>2</sub>O to 10  $\mu\text{L}$ . The reaction program was set up as follows: 95°C predenaturation for 3 min, followed by 40 cycles of 95°C for 10 sec and 60°C for 30 sec; moreover, fluorescence was quantified at 60°C. Samples with a cycle threshold (Ct) less than 35.0 were considered to be positive.

### Validation With Clinical Samples

To further verify the feasibility of RPA-*Pf*Ago in detecting MS in field samples, the collected clinical samples were extracted by using the thermal lysis method for nucleic acid detection via the RPA-*Pf*Ago assay, and qPCR was simultaneously used for validation. The

consistency between the 2 methods was compared and analyzed.

### Statistics and Analysis

The figures were drawn by using GraphPad Prism and Adobe Illustrator 2020. Data were analyzed with GraphPad Prism version 5.0 software (GraphPad Software Inc., San Diego, CA) using 1-way analysis of variance (ANOVA). Values are indicated as the means  $\pm$  SEMs. These values were significantly different compared to the control group. N = 3 technical replicates, \* $P < 0.05$ , \*\* $P < 0.01$ , \*\*\* $P < 0.001$ , \*\*\*\* $P < 0.0001$ .

## RESULTS

### Mechanism of the RPA-*Pf*Ago Detection Method

Figure 1A shows the complete process of detecting MS via the RPA-*Pf*Ago method. RPA performs exponential amplification of part of the heat shock ATP-dependent protease gene sequence when MS is present in the sample. The cleavage activity of *Pf*Ago targeted amplification products is obtained under the guidance of gDNA, which is complementary paired with the sequence to cleave at a specific position. The 5' phosphorylated ssDNA from the initial cleavage as secondary gDNA can guide *Pf*Ago for secondary cleavage. Moreover, the cutting substrate is a signal-producing molecular beacon with a hairpin structure, and the FAM fluorescence and BHQ1 quenching groups are modified at both ends. Secondary gDNA released by the first cleavage is complementary to the sequence of the circular portion, which directs *Pf*Ago to cut the molecular beacon and release the FAM fluorophore (Figure 1B). The fluorescence signal can be detected via a fluorescence detector or observed under UV light and blue light.

### RPA Primer Screening

To achieve efficient cleavage of *Pf*Ago, it is necessary to screen RPA primers for efficient amplification. Three forward and 3 reverse primers were designed and combined in pairs, thus resulting in a total of 9 combinations for MS RPA primer screening. Figure 2 shows that the band amplified by F3R1 is brighter than the other bands from other primers and is also free of stray bands; moreover, the fragment size was 134 bp. This set of primers was selected for RPA amplification of MS.

### gDNA Screening

In RPA-*Pf*Ago detection, gDNA is essential to guide *Pf*Ago to specifically recognize and cleave the target sequences, and the sequence of the molecular beacon is also determined by the first cleavage. In the amplified sequence of primer F3R1, a 59 bp ssDNA was synthesized as the target, and a total of 8 complementary



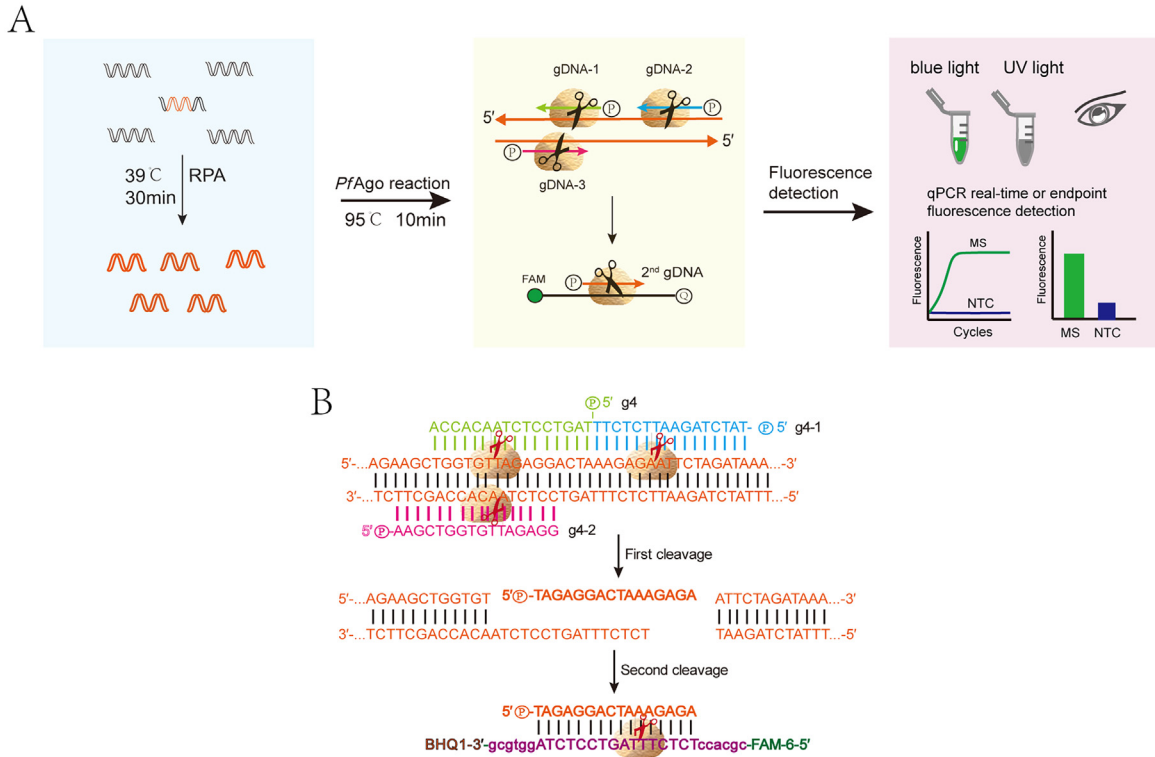


**Figure 1.** Schematic of the RPA-*PfAgo* assay in the detection of MS. (A) The specific process of MS detection by using the RPA-*PfAgo* method. (B) *PfAgo* “dual-step” cleavage under the guidance of gDNA. The *PfAgo* nuclease is shown as a brown mass. Abbreviations: FAM, fluorophore; P, phosphorylation; Q, BHQ1 quencher.

16 bp gDNA were designed every 4 bases with 5'-phosphorylation (Figure S1). As shown in Figure 3A, g4, g5, and g6 almost completely cut the ssDNA (Figure 3A), thus showing good guidance for *PfAgo* cleavage of ssDNA; finally, g4 was selected.

To compare the cleavage efficiency of different combinations of gDNA, 2 gDNA were designed (g4-1 and g4-2). *PfAgo* reactions containing 1 gDNA (g4), 2 gDNAs (g4 and g4-1), or 3 gDNAs (g4, g4-1, and g4-2) were added to cut the RPA amplification products. The fluorescence signal results showed that the fluorescence of the 3 gDNAs was higher than 1 gDNA and 2 gDNAs (Figure 3B).

### Optimization of the RPA-*PfAgo* Reaction

To determine the volume of RPA amplified product in the *PfAgo* cleavage reaction, 1–6  $\mu$ L of product was added. The results showed that an inappropriate volume

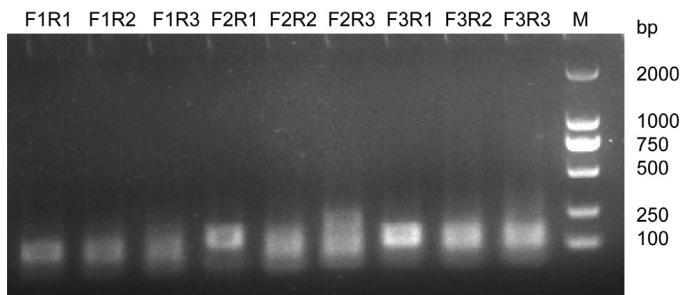


**Figure 2.** Primer screening via RPA. The amplification products of the 9 primer combinations were analyzed on agarose gels.

of RPA product was not conducive to *PfAgo* cleavage (Figure S2), moreover, when RPA product was added to 3  $\mu$ L and 4  $\mu$ L, the cleavage efficiency was higher and do not appear to be particularly different, a smaller RPA dose of 3  $\mu$ L was selected for testing.

*PfAgo* can utilize divalent cations to cleave the target mediated by gDNA. In this study,  $Mn^{2+}$  and  $Mg^{2+}$  were separately added to the *PfAgo* reaction and compared. The concentrations of  $Mn^{2+}$  and  $Mg^{2+}$  were initially separately optimized. Different concentrations of  $Mn^{2+}$  (0.0625, 0.125, 0.25, 0.5, and 1 mM) and  $Mg^{2+}$  (2.5, 5, 7.5, and 10 mM) were tested, and the endpoint signals demonstrated that 2.5 mM was the best concentration (Figure 4A). However, the concentration of  $Mg^{2+}$  from 2.5 mM to 10 mM showed little difference (Figure 4B). Moreover, it can be observed from the fluorescence curves that the sample with  $Mg^{2+}$  reaches a plateau at 10 min, whereas  $Mn^{2+}$  still did not reach a plateau at 30 min (Figure 4C). Therefore, 2.5 mM  $Mg^{2+}$  was used for the *PfAgo* reaction.

The concentrations of *PfAgo* and gDNA in the RPA-*PfAgo* reaction were optimized. Six concentrations of *PfAgo* ranging from 0 to 2.56  $\mu$ M were tested. Figure 5B shows that the efficiency of the reaction was significantly improved with the increased of *PfAgo* but decreased when the concentration reached 2.56  $\mu$ M. The highest cleavage efficiency was achieved when the concentration of *PfAgo* was 0.64  $\mu$ M and 1.28  $\mu$ M by observing the fluorescence signal; furthermore, 0.64  $\mu$ M was selected for the subsequent tests (Figure 5A). Five concentrations of gDNA were selected, and the fluorescence signal was similar (between 31.5 and 252 nM) (Figure 5C),

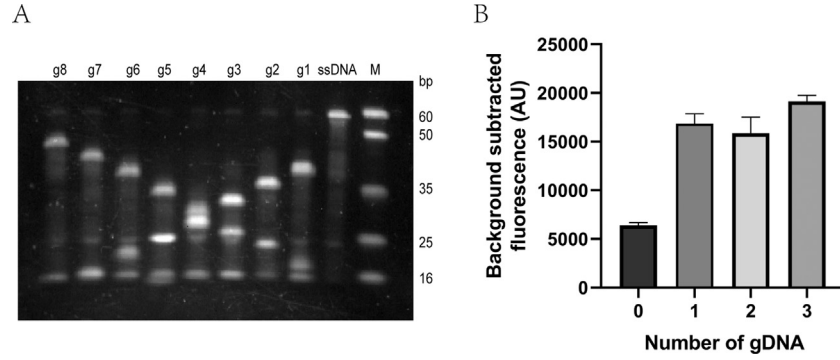


**Figure 3.** gDNA screening. (A) Eight gDNA guide *PfAgo* cleavage ssDNA were analyzed on PAGE gels. (B) Fluorescence intensity of RPA-*PfAgo* under the guidance of 0, 1, 2, and 3 gDNAs, respectively.

whereas the fluorescence curve demonstrated the time to reach the plateau shortened as the gDNA concentration increased (Figure 5D). When the concentration was 126 nM, it was not changed; therefore, 126 nM gDNA was selected as the optimal concentration.

### Sensitivity and Specificity of the RPA-*PfAgo* Method

To evaluate the sensitivity of the established RPA-*PfAgo* method, the recombinant plasmid pMD-19T-ATP at different dilution concentrations of  $2 \times 10^6$  to  $1 \times 10^0$  copies/ $\mu$ L was used as a template for detection.

As shown in Figure 6A, the detection limit of the RPA-*PfAgo* method was 2 copies/ $\mu$ L, which was 100 times higher than that of qPCR (Figure S3). When the tube was observed under UV or blue light, the sensitivity was 2 copies/ $\mu$ L (Figure 6B).

To evaluate the specificity of the RPA-*PfAgo* method, common clinical pathogens such as *S. aureus*, *E. coli*, *Salmonella*, KPn, MG, and MGC were used for the detection of specificity. Significant fluorescence signals could be observed in MS and MS-H (Figure 6C), and there was no cross-reaction with other pathogens, which indicated that the established method had high specificity. The same result was obtained by observing the reaction tubes under UV or blue light (Figure 6D).

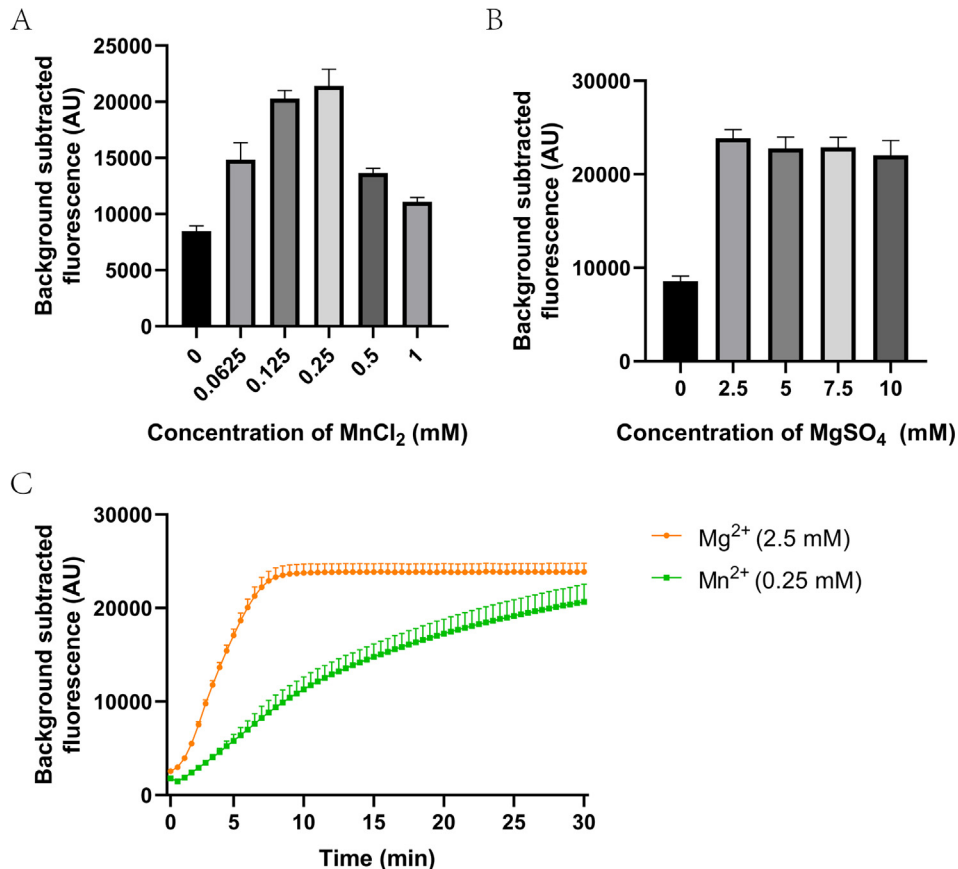


**Figure 4.** Screening of RPA-*PfAgo* divalent cations. (A and B) Optimization of different concentrations of  $Mn^{2+}$  and  $Mg^{2+}$ . (C) Fluorescence curves of  $Mn^{2+}$  and  $Mg^{2+}$ .

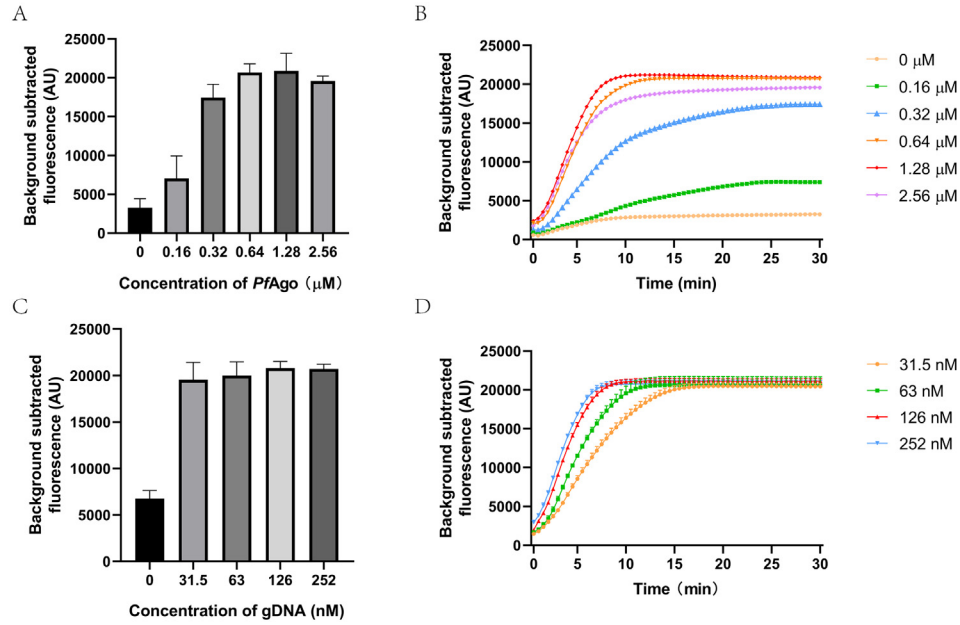


**Figure 5.** Optimization of the components for the RPA-*PfAgo* reaction. (A and C) Identification of the optimum concentrations of *PfAgo* and gDNA. (B and D) Fluorescence curves of different concentrations of *PfAgo* and gDNA.

## Examination of Clinical Samples

To evaluate whether RPA-*PfAgo* can be used to accurately detect clinical samples, 31 swab samples were simultaneously collected and detected via the optimized RPA-*PfAgo* and qPCR methods. A total of 21 positive samples and 10 negative samples were detected by using RPA-*PfAgo* (Figure 7A), and the captured image results under UV and blue light coincided with the fluorescence results (Figure 7C). The results were completely consistent via qPCR verification (Figure 7B). Furthermore, it is worth noting that the CT values of clinical samples such as 4 and 8 were less than but close to 35, whereas RPA-*PfAgo* was eventually effectively detected, thus

indicating the high sensitivity of the method in detecting MS.

## DISCUSSION

In 1954, Olson et al. (1954) and Wills (1954) first reported MS as an unidentified organism that causes synovitis in chickens. However, it was not until 1960 that the etiology of the disease was recognized. MS can be horizontally and vertically spread; additionally, all varieties and ages can be infected, and chicks are more susceptible than adults. The surface antigen of MS is prone to mutate, which leads to its escape from host

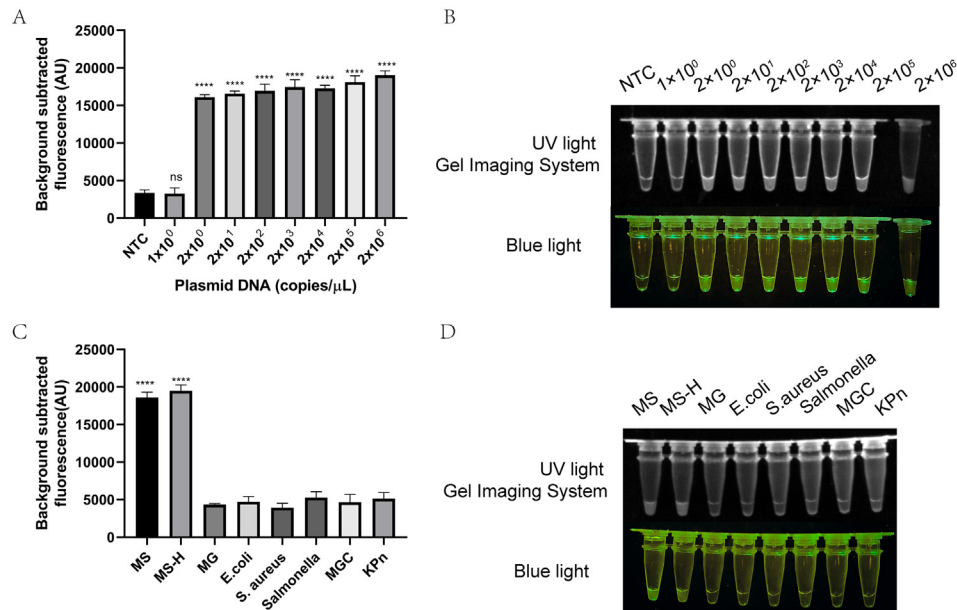


**Figure 6.** Sensitivity and specificity of the RPA-*PfAgo* reaction. (A and B) End-point fluorescence values of RPA-*PfAgo* sensitivity; the images were captured under UV light and blue light. (C and D) Specificity evaluation of RPA-*PfAgo* detection MS; the pictures were photographed under UV light and blue light. NTC: no template control. Error bars represent SEM; n = 3, \*\*\*\*  $P < 0.0001$ .

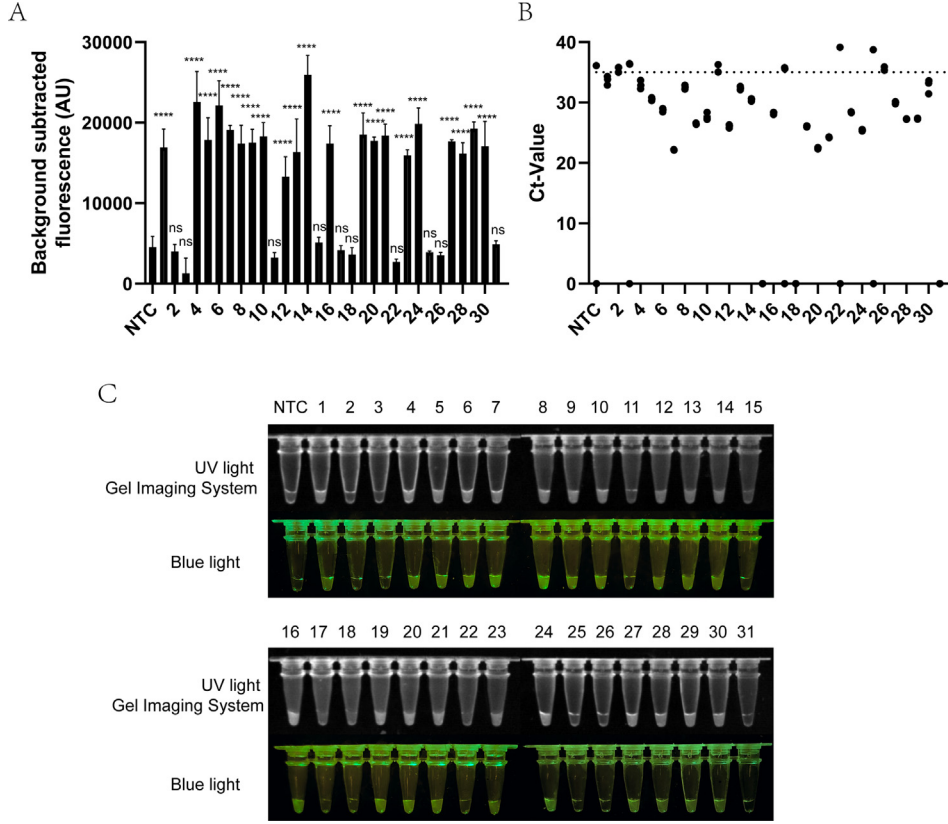


**Figure 7.** Clinical sample validation with RPA-*PfAgo* and qPCR. (A) A total of 31 clinical samples were detected by using RPA-*PfAgo*. (B) The clinical samples were tested via qPCR. (C) UV and blue light images of the sample were photographed. NTC: no template control. Error bars represent SEM;  $n = 3$ , \*\*\*\* $P < 0.0001$ .

immune recognition. Due to the lack of a cell wall, there is an inherent resistance to antibiotics acting on the cell wall, and the overuse of antibiotic treatments will easily lead to the emergence of antimicrobial resistance, which elicits challenges to controlling the spread of MS (Landman, 2014). Currently, the commonly used serological methods have low sensitivity and poor specificity. PCR-based molecular biological methods require more expensive instruments and equipment and skilled operators, among other conditions. Therefore, there is an urgent need to exploit an accurate and rapid nucleic acid-based MS detection method that is conveniently used in the field.

*PfAgo* is a nuclease with multiturnover activity that has begun to come into focus in recent years. The method of *PfAgo* combined with LAMP, RPA, and ligase chain reaction to detect COVID-19 has been established, and it has been shown that *PfAgo* can eliminate false-positives generated by isothermal amplification (Wang et al., 2021b; Xun et al., 2021a; Zhao et al., 2022). In the detection method based on *PfAgo*, gDNA is specific to the amplification product, and the cleavage product is specific to the molecular beacon. This step-by-step cleavage feature further ensures specificity (Enghiad and Zhao, 2017; Fu et al., 2019). In addition, gDNA is flexible and does not require specific motifs (such as the PAM motif required by Cas nuclease) for activation (Li et al., 2023). With short gDNA as the guide, compared with RNA, the cost is lower, and it is not easily degradable; additionally, it is easy to preserve.

When the substrates modified by different fluorophores are simultaneously present in a reaction, they are cleaved by *PfAgo* under the guidance of specific gDNA to produce fluorescent signals, which can be applied to simultaneously detect multiple targets.

The commonly used targets are the hemagglutinin-encoding gene *vlhA*, 16S rRNA gene, intergenic spacer region, or 23S rRNA gene in MS detection (Garcia et al., 1996; Hong et al., 2004; Ramírez et al., 2006; Sprygin et al., 2010). However, via sequence alignment and reference to related articles (Yang et al., 2019), more conserved heat shock ATP-dependent protease genes serve as the detection targets. The specificity tests showed that only MS and MS-H were detected by using RPA-*PfAgo*, with no cross reactions with other common pathogens. Furthermore, the primer design was reasonable, and the method had strong specificity.

*PfAgo* can use divalent cations (such as  $Mn^{2+}$  and  $Co^{2+}$ ) to cleave the target mediated by gDNA,  $Mn^{2+}$  was the most commonly used metal ion and proved to be better than  $Co^{2+}$  (Swarts et al., 2015; He et al., 2019). In this study, we found that  $Mg^{2+}$  can also be utilized by *PfAgo* to improve the reaction efficiency through experiments compared with  $Mn^{2+}$ , and the reaction time of *PfAgo* was shortened from 30 to 10 min. It has been reported that the cleavage efficiency of different numbers of gDNA also varies (He et al., 2019; Wang et al., 2021a). In the SPOT system, the cleavage efficiency of the detection reaction containing 3 gDNAs was improved, and the fluorescence value was 2-3 times



higher than that of 2 gDNAs (Xun et al., 2021a). Through carefully designed and screened gDNA and by comparing different combinations of gDNAs, 3 gDNAs were finally selected.

Through the optimization of the reaction conditions, RPA products can be directly used as templates for the *PfAgo* reaction, and nucleic acid detection can be completed in 40 min. The entire operation only requires a constant temperature heater and blue light instrument. Yang et al. (2023) and Zhao et al. (2022) established the RPA-*PfAgo* detection method which required the purification of RPA products; moreover, the *PfAgo* reaction required 30 min. In comparison, the operation and detection times were further simplified in this study.

## CONCLUSION

In summary, we have established a novel method that combines RPA with *PfAgo* for the detection of MS. The sensitivity of RPA-*PfAgo* is 2 copies/ $\mu$ L, and it does not cross-react with other pathogens. Additionally, simple operation and no need for precision instruments, which is helpful for the clinical detection of MS. This method is complementary to detection research based on *PfAgo* and is expected to be extended to food safety, pathogen detection, antibiotic resistance detection, and other fields.

## ACKNOWLEDGMENTS

This study was supported by the Local Innovative and Research Teams Project of Guangdong Pearl River Talents Program (Grant No. 2019BT02N054).

## DISCLOSURES

The authors declare no competing interests.

## SUPPLEMENTARY MATERIALS

Supplementary material associated with this article can be found in the online version at doi:10.1016/j.psj.2023.103244.

## REFERENCES

- Bashashati, M., and F. Sabouri. 2022. Development of two novel SYBR green-based quantitative PCR assays for detection and quantification of *Mycoplasma gallisepticum* and *Mycoplasma synoviae*. *Turk. J. Vet. Anim. Sci.* 46:226–234.
- Bozorgmehrifard, M., H. Hosseini, N. Sheikhi, and S. Charkhkar. 2018. Molecular detection of *Mycoplasma synoviae* from backyard and commercial turkeys in some parts of Iran. *Arch. Razi. Inst.* 73:79–85.
- Chen, W., L. Qiu, T. Luo, Z. Lu, X. Wang, Q. Hong, J. Luo, L. Ma, Y. Wang, and Y. Dong. 2023. Novel nucleic acid detection for human parvovirus B19 based on *Pyrococcus furiosus* Argonaute protein. *Viruses* 15:595.
- Enghiad, B., and H. Zhao. 2017. Programmable DNA-guided artificial restriction enzymes. *ACS Synth. Biol.* 6:752–757.
- Fu, L., C. Xie, Z. Jin, Z. Tu, L. Han, M. Jin, Y. Xiang, and A. Zhang. 2019. The prokaryotic Argonaute proteins enhance homology sequence-directed recombination in bacteria. *Nucleic Acids Res.* 47:3568–3579.
- Garcia, M., M. W. Jackwood, M. Head, S. Levisohn, and S. H. Kleven. 1996. Use of species-specific oligonucleotide probes to detect *Mycoplasma gallisepticum*, *M. synoviae*, and *M. iowae* PCR amplification products. *J. Vet. Diagn. Invest.* 8:56–63.
- He, R., L. Wang, F. Wang, W. Li, Y. Liu, A. Li, Y. Wang, W. Mao, C. Zhai, and L. Ma. 2019. *Pyrococcus furiosus* Argonaute-mediated nucleic acid detection. *Chem. Commun.* 55:13219–13222.
- Hong, Y., M. Garcia, V. Leiting, D. Bencina, L. Dufour-Zavala, G. Zavala, and S. H. Kleven. 2004. Specific detection and typing of *Mycoplasma synoviae* strains in poultry with PCR and DNA sequence analysis targeting the hemagglutinin encoding gene *vlhA*. *Avian Dis.* 48:606–616.
- Kaboudi K, J. A. 2019. *Mycoplasma synoviae* infection in layers: diagnosis and control measures: a review. *Arch. Vet. Med.* 12:63–82.
- Kleven, S. H. 1975. Antibody response to avian mycoplasmas. *Am. J. Vet. Res.* 36:563–565.
- Kleven, S. H. 2008. Control of avian mycoplasma infections in commercial poultry. *Avian Dis.* 52:367–374.
- Kleven, S. H., and N. Ferguson-Noel. 2008. *Mycoplasma synoviae* infection. *Dis. Poult.* 12:845–856.
- Kursa, O., G. Woźniakowski, G. Tomczyk, A. Sawicka, and Z. Minta. 2015. Rapid detection of *Mycoplasma synoviae* by loop-mediated isothermal amplification. *Arch. Microbiol.* 197:319–325.
- Landman, W., and A. Feberwee. 2004. Aerosol-induced *Mycoplasma synoviae* arthritis: the synergistic effect of infectious bronchitis virus infection. *Avian Pathol.* 33:591–598.
- Landman, W. J. 2014. Is *Mycoplasma synoviae* outrunning *Mycoplasma gallisepticum*? A viewpoint from the Netherlands. *Avian Pathol.* 43:2–8.
- Lauerman, L. H., F. J. Hoerr, A. R. Sharpton, S. M. Shah, and V. L. van Santen. 1993. Development and application of a polymerase chain reaction assay for *Mycoplasma synoviae*. *Avian Dis.* 37:829–834.
- Li, S.-Y., Q.-X. Cheng, J.-M. Wang, X.-Y. Li, Z.-L. Zhang, S. Gao, R.-B. Cao, G.-P. Zhao, and J. Wang. 2018. CRISPR-Cas12a-assisted nucleic acid detection. *Cell Discov.* 4:20.
- Li, Y., D. Liao, J. Kou, Y. Tong, L. C. Daniels, S. Man, and L. Ma. 2023. Comparison of CRISPR/Cas and Argonaute for nucleic acid tests. *Trends Biotechnol.* 41:595–599.
- Luciano, R. L., A. L. Cardoso, G. F. Stoppa, A. M. Kanashiro, A. G. de Castro, and E. N. Tessari. 2011. Comparative study of serological tests for *Mycoplasma synoviae* diagnosis in commercial poultry breeders. *Vet. Med. Int.* 2011:304349.
- OIE, A. 2008. Manual of Diagnostic Tests and Vaccines for Terrestrial Animals. Office International des epizooties, Paris, France, 1092–1106.
- Olson, N., J. Bletner, D. Shelton, D. Munro, and G. Anderson. 1954. Enlarged joint condition in poultry caused by an infectious agent. *Poult. Sci.* 33:1075.
- Ramírez, A. S., C. J. Naylor, P. P. Hammond, and J. M. Bradbury. 2006. Development and evaluation of a diagnostic PCR for *Mycoplasma synoviae* using primers located in the intergenic spacer region and the 23S rRNA gene. *Vet. Microbiol.* 118:76–82.
- Sid, H., K. Benachour, and S. Rautenschlein. 2015. Co-infection with multiple respiratory pathogens contributes to increased mortality rates in Algerian poultry flocks. *Avian Dis.* 59:440–446.
- Song, J., J. W. Hegge, M. G. Mauk, J. Chen, J. E. Till, N. Bhagwat, L. T. Azink, J. Peng, M. Sen, and J. Mays. 2020. Highly specific enrichment of rare nucleic acid fractions using *Thermus thermophilus* Argonaute with applications in cancer diagnostics. *Nucleic Acids Res.* 48:e19.
- Sprygin, A. V., D. B. Andreychuk, A. N. Kolotilov, M. S. Volkov, I. A. Runina, N. S. Mudrak, A. V. Borisov, V. N. Irza, V. V. Drygin, and N. A. Perevozchikova. 2010. Development of a duplex real-time TaqMan PCR assay with an internal control for the detection of *Mycoplasma gallisepticum* and *Mycoplasma synoviae* in clinical samples from commercial and backyard poultry. *Avian Pathol.* 39:99–109.
- Swarts, D. C., J. W. Hegge, I. Hinojo, M. Shiimori, M. A. Ellis, J. Dumrongkulraksa, R. M. Terns, M. P. Terns, and J. Van Der Oost. 2015. Argonaute of the archaeon *Pyrococcus*



- furiosus* is a DNA-guided nuclease that targets cognate DNA. Nucleic Acids Res. 43:5120–5129.
- Wang, F., J. Yang, R. He, X. Yu, S. Chen, Y. Liu, L. Wang, A. Li, L. Liu, and C. Zhai. 2021a. PfAgo-based detection of SARS-CoV-2. Biosens. Bioelectron. 177:112932.
- Wang, L., R. He, B. Lv, X. Yu, Y. Liu, J. Yang, W. Li, Y. Wang, H. Zhang, and G. Yan. 2021b. *Pyrococcus furiosus* Argonaute coupled with modified ligase chain reaction for detection of SARS-CoV-2 and HPV. Talanta 227:122154.
- Wills, F. 1954. Preliminary report on transmission of an agent producing an arthritis in chickens. Progress Report 1674. Texas Agri. Exper. Sta., College Station, Texas.
- Xia, W., K. Chen, W. Liu, Y. Yin, Q. Yao, Y. Ban, Y. Pu, X. Zhan, H. Bian, and S. Yu. 2022. Rapid and visual detection of *Mycoplasma synoviae* by recombinase-aided amplification assay combined with a lateral flow dipstick. Poult. Sci. 101:101860.
- Xiao, X., A. Xu, J. Zhai, and M. Zhao. 2013. Combination of a modified block PCR and endonuclease IV-based signal amplification system for ultra-sensitive detection of low-abundance point mutations. Methods 64:255–259.
- Xiao, X., C. Song, C. Zhang, X. Su, and M. Zhao. 2012. Ultra-selective and sensitive DNA detection by a universal apurinic/apyrimidinic probe-based endonuclease IV signal amplification system. Chem. Commun. 48:1964–1966.
- Xun, G., Q. Liu, Y. Chong, X. Guo, Z. Li, Y. Li, H. Fei, K. Li, and Y. Feng. 2021b. Argonaute with stepwise endonuclease activity promotes specific and multiplex nucleic acid detection. Bioresour. Bioprocess. 8:1–12.
- Xun, G., S. T. Lane, V. A. Petrov, B. E. Pepa, and H. Zhao. 2021a. A rapid, accurate, scalable, and portable testing system for COVID-19 diagnosis. Nat. Commun. 12:2905.
- Yang, B., Z. Chen, Y. Zhang, Y. Song, and S. Zhao. 2019. Development of a duplex PCR assay for simultaneous detection of *Mycoplasma gallisepticum* and *Mycoplasma synovium*. Anim. Husb. Feed Sci. 40:12–15.
- Yang, L., B. Guo, Y. Wang, C. Zhao, X. Zhang, Y. Wang, Y. Tang, H. Shen, P. Wang, and S. Gao. 2023. *Pyrococcus furiosus* Argonaute combined with recombinase polymerase amplification for rapid and sensitive detection of *Enterocytozoon hepatopenaei*. J. Agric. Food Chem. 71:944–951.
- Ye, X., H. Zhou, X. Guo, D. Liu, Z. Li, J. Sun, J. Huang, T. Liu, P. Zhao, and H. Xu. 2022. Argonaute-integrated isothermal amplification for rapid, portable, multiplex detection of SARS-CoV-2 and influenza viruses. Biosens. Bioelectron. 207:114169.
- Zhao, C., L. Yang, X. Zhang, Y. Tang, Y. Wang, X. Shao, S. Gao, X. Liu, and P. Wang. 2022. Rapid and sensitive genotyping of SARS-CoV-2 key mutation L452R with an RPA-Pf ago method. Anal. Chem. 94:17151–17159.
- Zhou, W., L. Hu, L. Ying, Z. Zhao, P. K. Chu, and X.-F. Yu. 2018. A CRISPR–Cas9-triggered strand displacement amplification method for ultrasensitive DNA detection. Nat. Commun. 9:5012.